



FINITE ELEMENT SIMULATION OF Al-1.5wt%Fe SAMPLES PROCESSED BY LASER SURFACE REMELTING

Siliane Machado²

Kelly dos Santos²

Viviane Teleginski³

Elisangela dos Santos Meza⁴

Rudimar Riva⁵

Moisés Meza Pariona⁶

Abstract

Nowadays, the components of automobiles are predominantly made of light alloys such as aluminum and magnesium. Although the density of these materials allows considerable savings in weight and consequently, in fuel consumption, in most cases, it is necessary to modify the basic form of the metal at its surface. This can be done by laser surface treatment. The propose of this study was to develop a mathematical model of the heat transfer, based on the finite element method, in order to simulate the weld fillet by laser remelting of the alloy Al-1.5wt%Fe using Comsol Multiphysics and Thermo-Calc softwares. In this work, the thermal properties of the alloy were introduced as temperature dependent functions due to the high temperature variations and the phase changes in the material occurred during the treatment. The simulation was carried out to analyze the spatial distribution of temperatures in the weld fillet. The Nd: YAG laser parameters used for the experiments were: 600 W, continuous wave operation in the TEM₀₀ mode, scanning speed of 40 mm/min and the laser beam was defocused 3mm. The weld pool shapes were simulated and compared with the experimental result and these results were satisfactorily consistent.

Key words: Simulation; Al-Fe alloys; Laser remelting.

SIMULAÇÃO POR ELEMENTOS FINITOS PARA AMOSTRAS Al-1,5m%Fe PROCESSADAS POR REUSÃO SUPERFICIAL A LASER

Resumo

Atualmente, os componentes de automóveis são predominantemente feitos de ligas leves como alumínio e magnésio. Embora a densidade desses materiais permitam uma redução considerável de peso e, conseqüentemente, no consumo de combustível, na maioria dos casos, é necessário modificar a forma básica do metal em sua superfície. Isso pode ser feito por tratamento superficial a laser. O objetivo deste estudo é desenvolver um modelo matemático de transferência de calor, com base no método dos elementos finitos, para simular a superfície refundida por laser na liga Al-1.5 wt% Fe, utilizando os softwares Comsol Multiphysics e Thermo-Calc. As propriedades térmicas do material são introduzidas como funções dependentes da temperatura, devido às grandes variações de temperatura e mudanças de fase que ocorrem no material durante o tratamento. A simulação realizada analisou o histórico da distribuição espacial da temperatura na região irradiada. Os parâmetros do laser Nd: YAG utilizados para os experimentos foram: 600 W, operação de onda contínua no modo TEM₀₀, velocidade de varredura de 40 mm/min e com o feixe laser desfocado 3mm. Os perfis simulados refundidos foram comparados com os resultados experimentais, sendo que os resultados mostraram-se satisfatoriamente coerentes.

Palavras-chave: Simulação; Ligas Al-Fe; Refusão a laser.

¹ Technical contribution to 66th ABM Annual Congress, July, 18th to 22th, 2011, São Paulo, SP, Brazil.

² Graduanda de Licenciatura em Matemática, aluna de Iniciação científica pelo PIBIC/UEPG, da Universidade Estadual de Ponta Grossa - UEPG.

³ Tecnóloga em Processos de Fabricação Mecânica, Mestranda do Departamento de Engenharia e Ciência de Materiais da UEPG.

⁴ Mestre em Matemática, doutoranda da Faculdade de Engenharia Mecânica da UNICAMP.

⁵ Professor Doutor do departamento de Física do Instituto Tecnológico da Aeronáutica, CTA - São José dos Campos - SP

⁶ Professor Doutor da Pós Graduação de Engenharia e Ciência de Materiais da UEPG.



1 INTRODUCTION

High productivity with low cost is a major focus for the welding industry and its associated research community, especially in the welding of thick materials. Currently, electron beam welding and laser welding are the primary processes to join thick materials in a single pass. However, the bad gap bridging ability and high cost are the obvious disadvantages for both processes.⁽¹⁾

Laser welding has the advantage of localized heat, low distortion and rapid solidification, and is used in wide variety of material joining applications. Laser welding is performed either in conduction or in keyhole mode. In conduction mode, the applied power density is smaller and vaporization of work piece material is absent. Keyhole mode laser welding involves the application of very high power density creating a vapor filled cavity into the work piece that also helps in greater absorption of beam energy.⁽²⁾ An appropriate design for welding procedure requires a-priori knowledge of the peak temperature, weld thermal cycle and cooling rate. Due to high peak temperature and small weld pool size, real-time measurements of temperature and velocity fields, and the growth of weld pool are difficult in laser welding.⁽²⁾ Thus, the computational models, which can simulate temperature and velocity field in laser welding, is an ever demand.⁽²⁾

Thus, conduction heat transfer based models are often preferred to the convective heat transport based weld pool simulations for smaller weld pool sizes and joining processes involving rapid melting and solidification. The conduction heat transfer based weld pool models also find tremendous application in the calculations of weld distortion and residual stress,⁽²⁾ where the temperature field over a very large domain is of greater importance in comparison to its local variation in weld pool.

The combination of laser welding with pulsed gas metal arc welding (GMAW-P) forms Laser + GMAW-P hybrid welding which can not only enhance capability of the two processes, but also compensate the deficiencies of each individual. As applications become more widespread, there is growing need to understand the fundamental issues of this new welding process, such as the relationship between the numerous process parameters and the weld quality. For key factors determining the weld quality, the temperature history, thermal stress and distortion have significant effects on the microstructure and properties of weld joint. For example, residual stresses pose significant problems in the precision fabrication of structures because those stresses heavily induce brittle fracturing and degrade the buckling strength of welded structures.⁽³⁾ Therefore, predicting the magnitude and distribution of weld residual stresses and characterizing the effects of certain welding conditions on the residual stresses are of great significance for more widespread applications of Laser + GMAW-P hybrid welding. However, these advances are mostly associated with typical welding processes, such as arc welding or laser beam welding. For Laser + GMAW-P hybrid welding, which is increasingly applied in manufacturing industry, fundamental investigations involving mathematical modeling and associated experiments have been carried out only to a limited extent.⁽³⁾ Though some work has been conducted for modeling and simulation of heat and fluid flow in hybrid welding,⁽³⁾ there is still a lack of thermomechanical analysis of residual stresses and distortion for this new process.

Validated methods for predicting welding stresses and distortion are desirable because of the complexity of welding process which includes localized heating, temperature dependence of material properties, moving heat source, etc. Accordingly, finite element (FE) simulation has become a popular tool of the

prediction of welding residual stresses and distortion. Many investigators have developed analytical and experimental methods to predict welding residual stresses.⁽⁴⁾

As shown in Figure 1,⁽⁵⁾ laser welding is a non-contact fusion process. With laser beam, energy is concentrated directly in a small welding area. Consequently, the welding zone is very narrow and hardly distorted due to little heat influence. Compared to traditional processes, laser welding is of potential. Its non-contact, localized, and narrow heat zone can create high quality result. Common re-working and after-work procedure are no more required, which saves cost and labor. Till now, laser welding has been widely applied in various fields including automotive, microelectronics, aerospace, etc. Common types of lasers applied to welding include CO₂ gas laser, solid state laser (YAG type), and diode laser welding. CO₂ laser uses a mixture of high purity carbon dioxide with helium and nitrogen as the medium, producing infrared length-wave of 10.6 micro-meters. Argon or helium is additionally used to prevent oxidation. YAG laser takes advantage of a solid bar of yttrium aluminum garnet doped with neodymium as the medium, whose infrared is only 1.06 micro-meters. Diode laser is mostly based on the conversion between high electrical to optical powers.

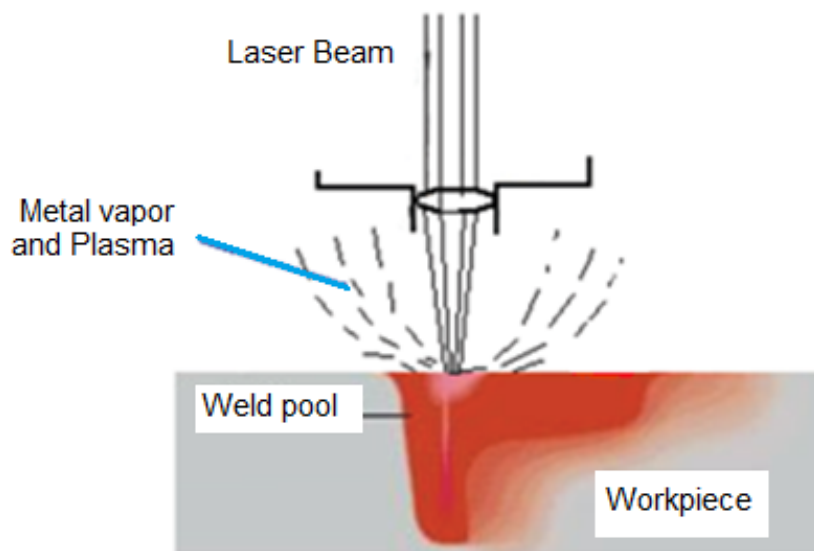


Figure 1. Simple laser welding process.⁽⁶⁾

The purpose of this study is to numerically simulate the weld fillet by the laser remelting process applying the finite element method. The effect of convection is taken into account as boundary condition. In this work also the microstructural analysis was carried out using optical microscopy and SEM of laser treated Al-1.5wt%Fe samples. Finally, the experimental results and simulations were compared.

2 MATERIALS AND METHODS

The alloy Al-1.5wt%Fe was cast with commercially pure raw materials, in the laboratories of UNICAMP and it was cut in small samples. The phase diagram Al-Fe alloy is show in Figure 2. The obtained material was analyzed with X-ray, and its composition is observed at Table 1.

Table 1 Chemical composition (%wt.)

Fe	Cu	Ni	Si	Al
----	----	----	----	----

1.5	0.06	0.03	0.06	Balance
-----	------	------	------	---------

Afterwards, they were sand blasted and the upper surface of the samples was covered with several weld fillets by the remelting process with fiber laser doped with Ytterbium (Nd: YAG). For this purpose the used parameters of the laser beam were scan velocity of 40 mm/min with 600 W of power. The average separation between the weld fillets was 300 micro-meters. The scheme about the welding system is shown in Figure 3. In Figure 4 the surface of a sample treated with laser is shown. Samples have been cut and prepared by metallographic techniques, with diamond paste (1 μ m) and colloidal silica. These were etched in a solution HF 0.5% and observed by optical microscopy (OM) and scanning electron microscope (SEM), Shimadzu SSX-550.

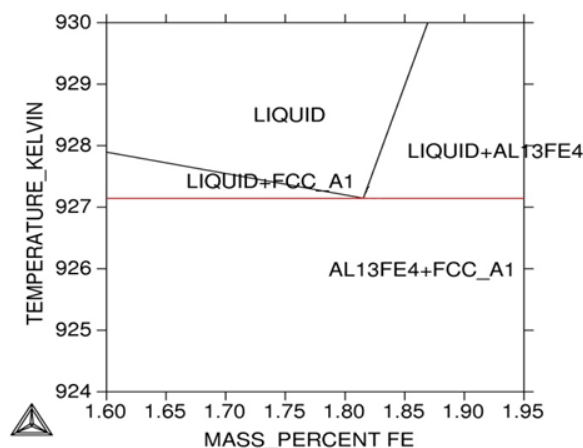


Figure 2. Phase diagram to Al-Fe.⁽⁶⁾

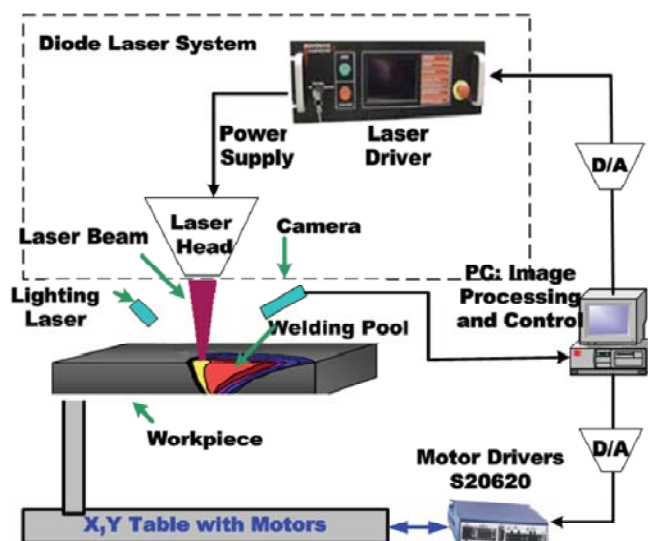


Figure 3. Standard vision sensor based automatic diode laser welding system.⁽⁵⁾



Figure 4. Micrography of the alloy Al-1.5wt%Fe treated by laser surface remelting processes.

3 MATHEMATICAL MODELING

A 3D Cartesian coordinate system was set on the workpiece, being the x-axis along the moving welding direction with v speed, z-axis along the thickness direction and the origin located on the workpiece surface. Its dimensions are show in Figure 5. The transient heat conduction equation [7] (Eq. 1) is written as

$$\rho \frac{\partial(c_p T)}{\partial t} = \frac{\partial}{\partial x} \left(k \frac{\partial T}{\partial X} \right) + \frac{\partial}{\partial y} \left(k \frac{\partial T}{\partial y} \right) + \frac{\partial}{\partial z} \left(\frac{\partial T}{\partial z} \right) + (1 - r_f) I_0 \exp \left(-\frac{(v \cdot t)^2}{a^2} \right) \exp(-\delta z) \quad (\text{eq. 1})$$

where x , y and z are the vertical, axial and horizontal coordinates, respectively, ρ is the density, c_p is the specific heat, k the thermal conductivity, r_f the surface reflectivity, I_0 is the laser peak intensity, δ the absorption depth, t is time, and “ a ” is a Gaussian parameter. It should be noted that the laser power intensity distribution at the workpiece surface is assumed as a Gaussian form. The laser parameters used in this work are shown in Table 2.

Table 2. Laser parameters

Welding speed	40 mm/s
Real Power of laser	600 W
Reflectivity (r_f)	0.63 %
Radius of the Gaussian distribution (a)	0.3 mm
Laser peak intensity (I_0)	$6.8 \times 10^9 \text{ W/m}^3$
Absorption depth (δ)	negligible

The thermophysical properties were considered dependent with the temperature for to calculate the specific heat. For to calculate them, they were associated with the solidified fraction (Figure 5a) and enthalpy (Figure 5b).

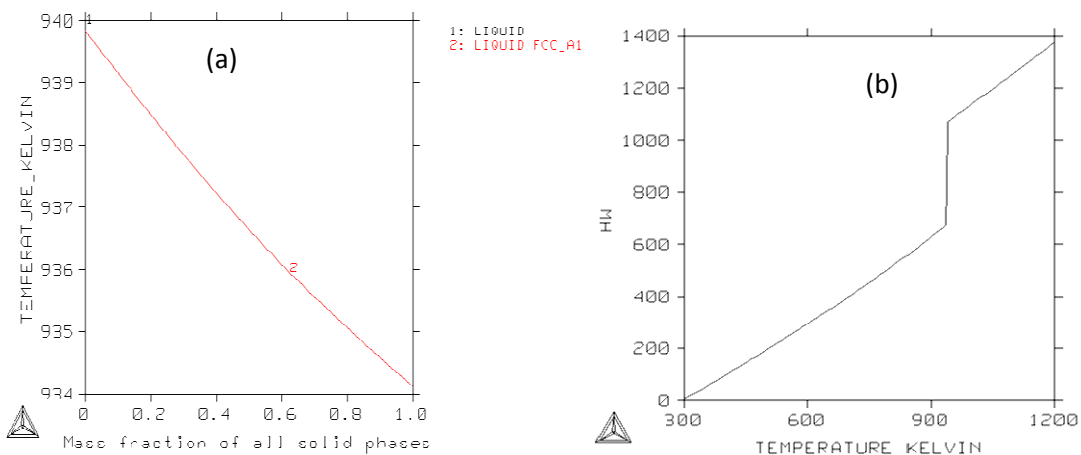


Figure 5. For Al-1.5wt%Fe alloy, (a) solidified fraction and (b) enthalpy.⁽⁶⁾

The boundary conditions and the corresponding heat flux expressions are represented in Figure 6, where the upper and lower surfaces of the aluminum sample lose heat due to natural convection and surface to ambient radiation.⁽⁷⁾

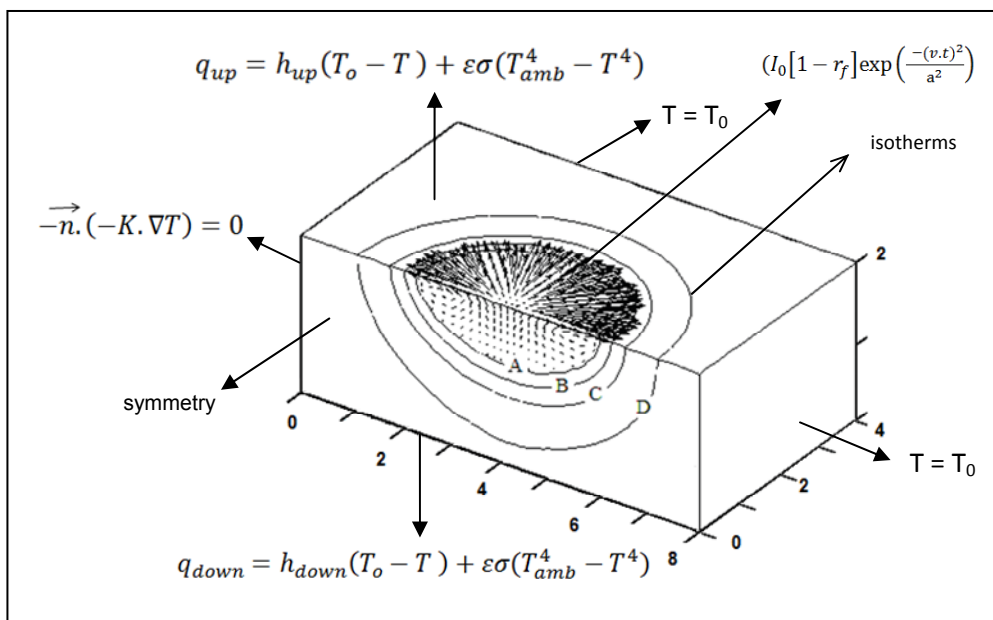


Figure 6. A 3D computational view of temperature and isotherms distribution. The boundary conditions are indicated on each surface of the geometry.

The mesh applied on the geometry is shown in Figure 7(a) and the refinement in the interest area where the laser beam is focus, is shown in Figure 7 (b).

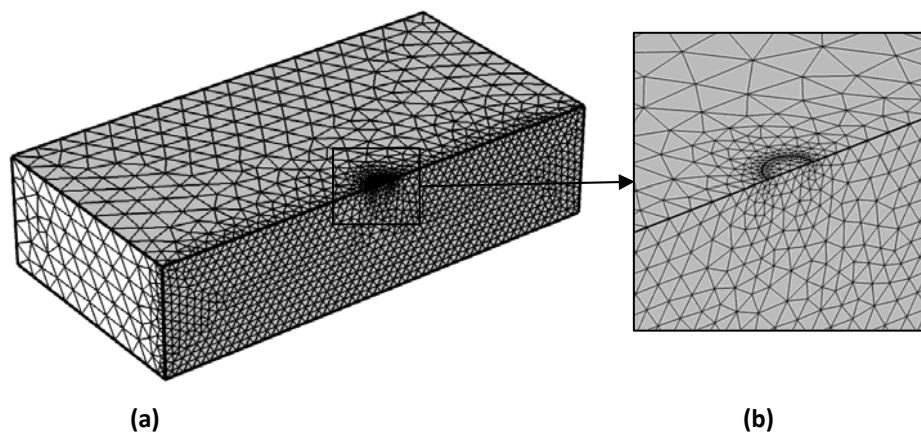


Figure 7. Finite element mesh at (a) work-piece and (b) details of the refinement where the laser beam is focus.

Some simplifying assumptions were adopted for the development of the numerical model. They concern on: (i) the reduction of field study by making use of symmetry. The thermal history of only one half of the assembly was predicted. (ii) Simulation was made considering that the laser beam moves at constant speed. It is also assumed (iii) an uniform power distribution in the keyhole, (iv) an isotropic thermal behavior during welding. (v) In this simulation only one weld fillet was considered, even when in the performed experiments one surface of the workpiece was covered by several weld fillets, and simulate this condition will be part of future works.

4 RESULTS

A thermal simulation was conducted to analyze the spatial temperature distribution in the laser irradiated region using the finite element method (FEM). Figures 8(a) and (b) show the distribution of thermal fields in a 3D view. The red region represents the melt pool and the isotherms are not distributed uniformly. On the left side of the melt pool, there is greater heat diffusion because the laser beam had already passed in that region. But in the right side the scattering is small due to the short time of interaction of the sample with the laser beam. Figure 8(c) show the hot spot magnification, indicating the temperatures reached in some fields.

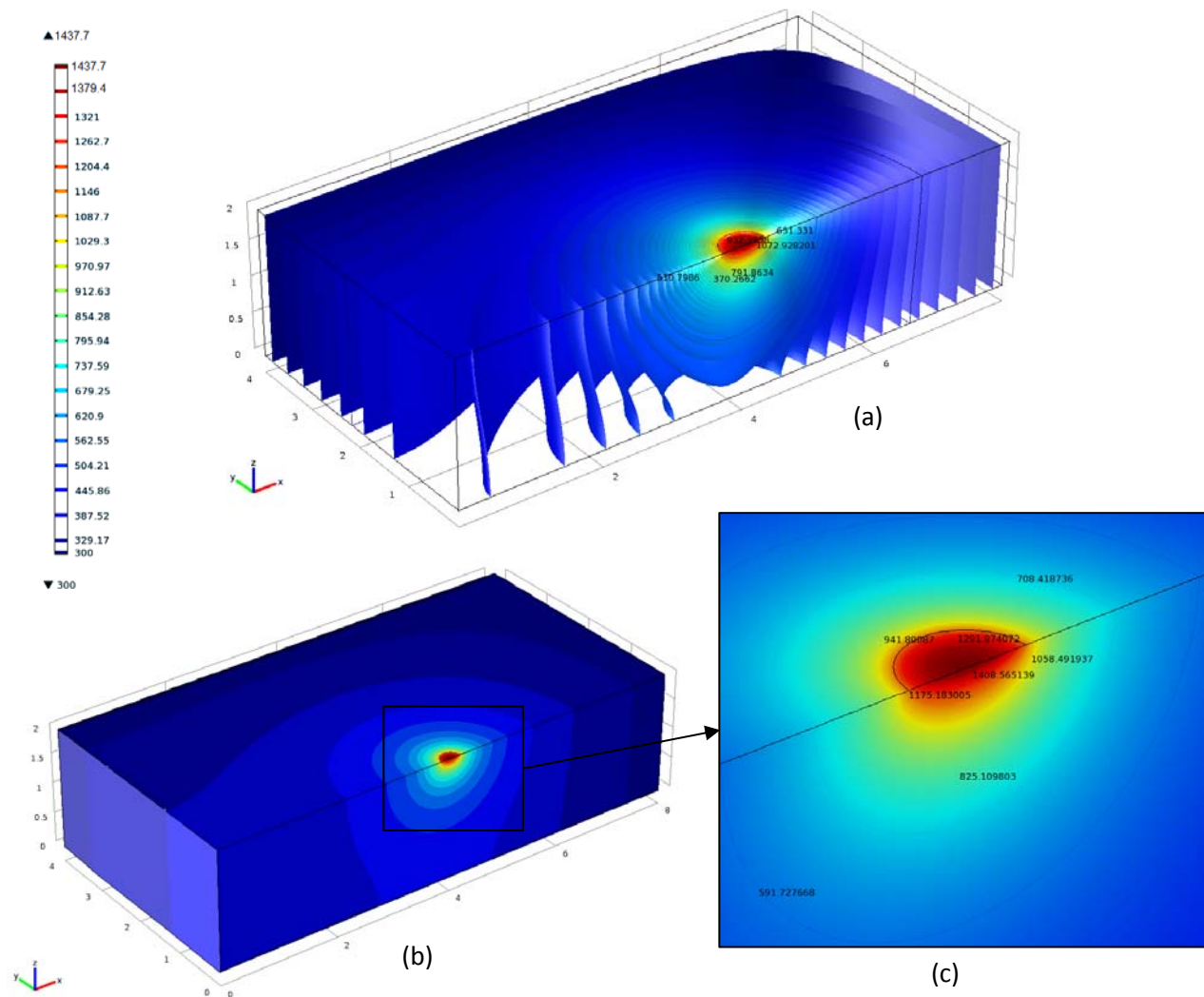


Figure 8. Laser remelting of Al-1.5wt%Fe alloy (a) and (b) distribution of thermal fields; (b) details of the isotherms in the weld pool and around it.

The simulation was confronted with the experimental results obtained for the Al-1.5wt%Fe alloy. Studies concerning the microstructure obtained due to the laser treatment were carry out. Figure 9 (a) show a cross-section micrography of the modified region produced by the laser remelting process and the unaffected substrate. Point defects, as microporosities, can also be observed in the micrography.

Figure 9 (b) shows a magnification of the interface between the marks originated by the melt pool and the thermally affected zone, which microstructure appears more refined. The magnified interface between the unaffected substrate and the thermally affected zone can be observed in Figure 9 (c). The substrate microstructure is shown in Figure 9 (d).

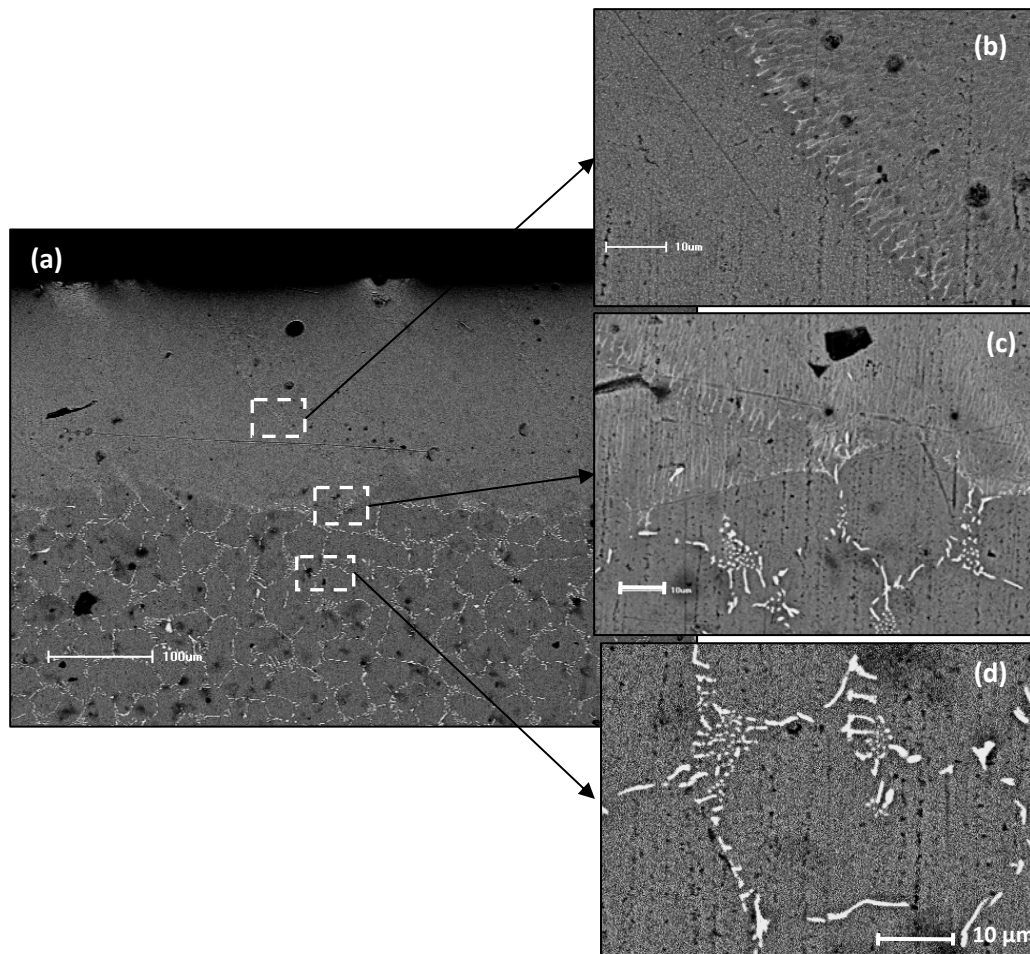


Figure 9. Cross-section microstructure of the sample treated by laser, showing: (a) the interface between the remelted region and substrate; (b) interface between the melt pool and thermally affected zone; (c) interface between thermally affected zone and substrate; and (d) substrate in the unaffected area.

To view in more details the interface between the melt pool and the thermally affected zone Figure 10(a) is presented and for highlight the interfaces, lines were drawn as Figure 10 (b) shows.

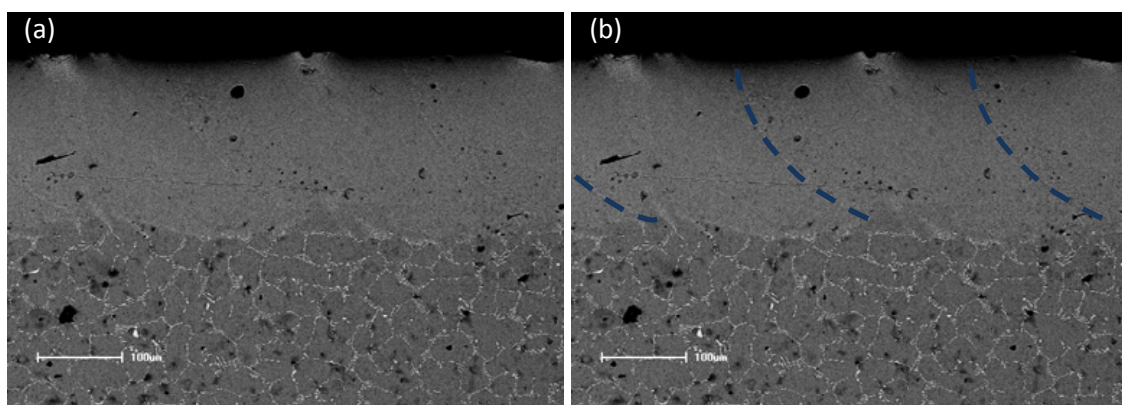


Figure 10. (a) Microstructure obtained by laser surface remelting, showing the formation of the weld pool shapes; (b) Drawn lines in the interface between the melt pool and the thermally affected zone.

In order to compare the simulation with the experiments results only one weld fillet was considered. The simulation of the surface covered with weld fillets is very complex and it will be held in the future.

The Figure 11 shows a comparison between the obtained result by SEM and simulation, where the temperatures of some isotherms are indicated. The depth of the welding pool was about 210 μm for 927 K.

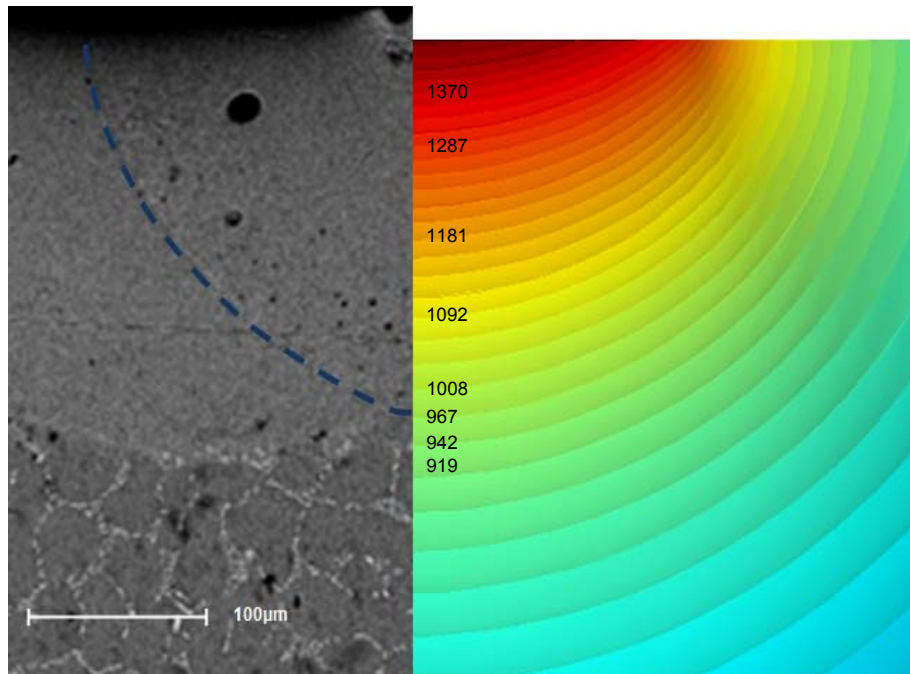


Figure 11. Comparison between the experimental sample and the numerical simulation in the cross-section view.

4 DISCUSSIONS

The simulation showed the distribution and the characteristics of the isotherms formed by the application of the laser in quantitative and qualitatively form, indicating its minimum and maximum temperatures. The laser beam is applied in a very located and small area, while the most part of the surface finds-itself in the environment. Due to this difference of area and temperature, laser remelting permits high rates of cooling and solidification. For illustrate this idea, the Figure 8 brings an enlargement of the melt pool and thermally affected region, showing in details the isotherms that are formed.

In Figure 9 (a) the protuberances can be observed in the places where the laser beam passed and this phenomenon occurs for laser treatments at low scan speeds (under 100 mm/min).⁽⁹⁾ Microstructural differences also showed in Figure 9 (a) indicated refinements of the treated zone. Due to the dimensions of the cellular morphologies in the substrate, it can be assumed that the size of the particles in the melt pool region must be much small than 10 μm , on this subject, some authors discuss that the aspect of these microstructures that is quite unusual is the formation of randomly oriented intercellular intermetallic dispersoids with diameters on the order of 50 nm in a microcellular matrix.^(10,11)

Even between the weld fillets, as shown in Figure 9 (b), a most refined microstructure is found. This is probably due to the double heating in the region. The



first one occurs when the weld fillet is been formed, the second when the next weld fillet is been formed, and its heat affect the preview melt pool.

The comparison of the simulated and the experiments can be observed at figure 10, where the interface of the melt pool and thermally affected zone are around 919 K e 942 K. Considering the melting temperature for pure aluminum, 933 K, and this being the maximum depth of the melt pool, there is agreement with simulated and experiments.

5 CONCLUSIONS

A transient three-dimensional of the heat transfer by numerical simulation of the laser remelting process was performed based on the finite element method, that permitted to predict temperature distributions in the weld fillet. Depth theoretical prediction of the melt pool provided by simulation is in agreement with experimental result of the laser remelting of the alloy Al-1.5wt%Fe samples. The experimental analysis also revealed different zones of refined microstructures in the laser weld fillet cross section. This study also permits to conclude that numerical simulation is a powerful tool to predict and interpret phenomena that are impossible to observe experimentally.

Constants

h_{up}	heat transfer coefficient for natural convection
h_{down}	heat transfer coefficient for natural convection
T_o	associated referred temperature
ε	surface emissivity
σ	Stefan-Boltzmann constant
T_{amb}	ambient air temperature
∇T	direction vector for temperature gradient

Acknowledgements

The authors acknowledge the financial support provided by CNPq (Brazilian Research Council) and Araucária Foundation (AF). To Dr. Milton D. Michel for the support with SEM.

REFERENCES

- 1 Zhao Y.B., Lei Z.L., Chen Y.B., Tao W.. A comparative study of laser-arc double-sided welding and double-sided arc welding of 6 mm 5A06 aluminum alloy. *Materials and Design*, v.32, p.2165–2171, 2011
- 2 Bag S., De A. Computational modelling of conduction mode laser welding process. *Laser Welding* edited by Dr. Na, X. Published by Sciyo, Rijeka-Croatia, 2010
- 3 Zhang T., Wu C.S., Qin G.L., Wang X.Y., Lin S.Y. Thermomechanical analysis for Laser + GMAW-P hybrid welding process. *Computational Materials Science*, v. 47, p. 848–856, 2010.
- 4 Zeng Z., Li X., Miao Y., Wu G., Zhao Z. Numerical and experiment analysis of residual stress on magnesium alloy and steel butt joint by hybrid laser-TIG welding. *Computational Materials Science* v.xxx, p.xxx–xxx, 2011. Article in press.



- 5 Na, X. Laser welding: techniques of real time sensing and control development. Laser Welding edited by Dr. Na, X. Published by Sciyo, Rijeka-Croatia, 2010.
- 6 Thermo-Calc Software, Stockholm, Sweden, 2010.
- 7 Handbook, COMSOL Multiphysics software, 2011.
- 8 Yilbas, B.S.; Arif, A.F.M.; Karatas, C., Raza, K. Laser treatment of aluminum surface: Analysis of thermal stress field in the irradiated region. Journal of Materials Processing Technology, v. 209, p.77–88, 2009.
- 9 BERTELLI, F. MEZA, E.S. GOULART P.R. CHEUNG N. RIVA, R. GARCIA, A. Laser remelting of Al- 1.5 wt%Fe alloy surfaces: numerical and experimental analyses. Optic and Lasers in Engineering, v. 49, p. 490-497, 2011.
- 10 Cotton J.D., Kaufman M.J. Microstructural evolution in rapid solidification Al-Fe alloys: An alternative explanation. Metallurgical Transaction A, v.22A, p.199-215, 1991.
- 11 Gilgien P., Zryd A., Kurz W. Microstructure selection maps for Al-Fe alloy. Acta metallurgica, v. 43, p.3477-3487, 1995.